*Proceedings of the Pakistan Academy of Sciences: B*
*Life and Environmental Sciences* 60(3): 549-555 (2023)

ISSN (Print): 2518-4261; ISSN (Online): 2518-427X
http://doi.org/10.53560/PPASB(60-3)834

Pakistan Academy of Sciences

Research Article

# Surfactant-Promoted Prussian Blue Analogues Fabricated Electrodes for Electrocatalytic Water Oxidation

**Sana Ibadat, Hafiza Tauseef Ashfaq, Ruqia, Muhammad Adeel Asghar, Ali Haider*, and Saqib Ali***

Department of Chemistry, Quaid-i-Azam University, 45320 Islamabad, Pakistan

**Abstract:** Prussian blue analogues (PBAs) have unique structural and chemical behaviour and therefore have applications in various fields of catalysis as energy conversion materials for storage devices and molecular sensing. Herein we focused on the in-situ synthesis of three PBAs comprising cobalt hexacyanoferrate (CoHCF), nickel hexacyanoferrate (NiHCF), and cobalt-nickel hexacyanoferrate (CoNiHCF) through cation i.e. cetyltrimethylammonium bromide (CTAB) assisted drop cast method. The electrocatalysts were characterized through a multitude of spectroscopic techniques and were tested for water oxidation study. It was found that among the three electrocatalysts, CoNiHCF showed comparatively better catalytic performance with an overpotential value of 570 mV (at 1 mA $cm^{-2}$)

**Keywords:** Prussian Blue Analogues, Coordination Polymers, Cationic Surfactants, Cetyltrimethylammonium bromide, Water Oxidation Studies

## 1. INTRODUCTION

We are heavily reliant on fossil fuels to meet the annual global energy demand [1]. However, the excessive burning of fossil fuels results in the emission of $CO_2$ into the atmosphere, which can be avoided by substituting non-toxic and renewable fuels for fossil fuels [2-3]. To convert solar energy into a usable form, the photovoltaic system has also emerged as a viable solution, but it still has significant drawbacks. As a result, finding a different source of energy is crucial [4-6]. Given all the options, hydrogen having the highest energy density and producing non-toxic byproducts is regarded as one of the most suitable energy sources [7]. Electrochemical water splitting is an intriguing method for producing hydrogen [6, 8]. However, oxygen evolution reaction (OER) has sluggish kinetics that needs more overpotential, and therefore, effective electrocatalyst that can reduce the activation energy, consequently, the overpotential of the reaction is required. The most common electrocatalysts utilized in the process are metal oxides based on Ir, Ru, and Pt [9-11]. However, their high cost and scarcity have significantly limited the usage of these metal oxides [11]. In the process of splitting water, several transition metals are also used as metal oxide electrocatalysts. First-row transition metal oxides, however, have several drawbacks, including the fact that metal oxide performance varies on different experimental conditions, such as morphology, temperature, etc [11]. Consequently, it is crucial to control them in order to obtain correct findings. Otherwise, it makes their applicability very challenging [11]. Additionally, the first-row transition metal oxides function best in an alkaline environment (Ph $\geq$ 13) but are less effective in acidic or neutral conditions [12]. Different non-oxide materials such as metal phosphides, sulphides, selenides, nitrides, based molecular-based organic metal-organic frameworks (MOFs), and polyoxometalates, etc. are known water oxidation catalysts (WOCs) with advantageous qualities, such as simplicity in synthesis, stability over a wide pH range, and durability during catalytic processes [13]. Among different coordination polymers, PBAs have been employed as heterogeneous electrocatalysts for OER [14]. The group of Galán-Mascarós have extensively studied the role of PBAs as WOCs

Received: January 2023; Revised: April 2023; Accepted: June 2023
*Corresponding Authors: Ali Haider <ahaider@qau.edu.pk>; Saqib Ali <saqibali@qau.edu.pk>

[15-18]. The group proved that PBAs are important electrocatalysts in water oxidation because of open metal active sites, the high porosity of the framework, and most importantly the easy oxidization of metal ions to their higher oxidation states [18]. The group of Karadas reported the preparation of amorphous PBAs through a novel synthetic route that exhibited high electrocatalytic water oxidation activity [4]. Recently we have reported the preparation of amorphous bimetallic PBAs following the pyridinium based surfactant assisted route to prove that surfactants play a significant impact on the film development (binder-free approach), better stability and charge transfer kinetics of OER [19]. We further extended the fabrication approach to electrodeposition method as well [20].

Herein, we examined the effect of a cationic surfactant on the electrocatalytic water oxidation performance of synthesized bimetallic and trimetallic PBA films. In the presence of cationic surfactant, PBA films have been deposited on the glassy carbon electrode (GCE). The fabricated electrode ultimately demonstrated a significant improvement in the electrochemical performance of synthesized catalysts toward OER.

## 2. MATERIALS AND METHODS

### 2.1. Chemicals

The chemicals that include sodium hexacyanoferrate (II) ($Na_4Fe(CN)_6$; HCF), sodium hydroxide (NaOH), and sodium nitrate ($NaNO_3$) were purchased from Sigma-Aldrich (St. Louis, MO, USA). For cobalt and nickel sources, the nitrate salts were used. Cetyl-trimethyl ammonium bromide (CTAB) as cationic surfactant and DMF as solvent was used. All the solutions were prepared in deionized water at room temperature.

### 2.2. Instrumentation

The Gamry Interface 1010E potentiostat/galvanostat is equipped with a standard three-electrode setup comprising platinum wire as a counter electrode, Ag/AgCl (3 M KCl) as a reference electrode, and modified glassy carbon (2 mm in diameter) as working electrode

The transmission spectrum of each powder sample was recorded in the frequency range of 4000 – 400 $cm^{-1}$ and performed on a Thermo Nicolet-6700 FT-IR spectrophotometer. Powdered X-ray diffraction (PXRD) analysis of the synthesized materials was recorded on a PANalytical X'pert instrument equipped with CuKα X-ray source (λ = 1.5418 Å) in the range of 20 to 80◦. Scanning electron microscopy (SEM) was carried out using FESEM (NOVA-600) coupled with Bruker EDX system at an accelerating voltage of 3 kV.

### 2.3. *In-situ* Synthesis of Catalyst on the Electrode Surface

Before modification of the GCE, it was initially washed with alumina powder slurry on a polishing pad. The electrode was dipped in acetone and sonicated for about 30 min to remove solid particles from the electrode surface if any. After sonication with acetone, it was sonicated with distilled water. Finally, it was dried in an oven.

To develop the corresponding PBAs films (i.e. of CoHCF, NiHCF, or CoNiHCF) films, a drop of surfactant in DMF was added onto the GCE surface using a micropipette. Once the electrode dried out, a 10 µL of 10 mM aqueous HCF and 15 mM aqueous corresponding metal salt solutions were added simultaneously (schematically presented in Figure 1).

## 3. RESULTS AND DISCUSSION

### 3.1. Synthesis and Characterization

The synthesis of PBAs through a surfactant-assisted mechanism is the key factor in generating an efficient electrocatalyst for OER in this work. The surfactants form hemimicelles onto the surface

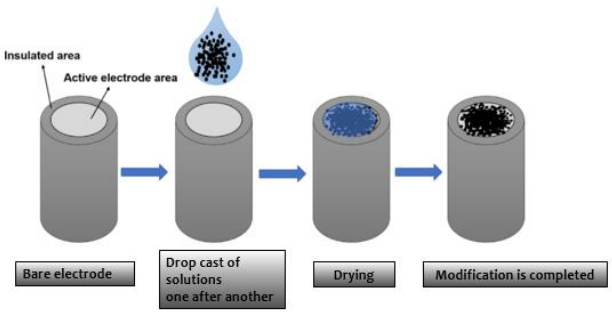


**Fig. 1.** Schematic presentation of electrode modification.

of the GCE such that the headgroups are exposed to the aqueous solution. This overall supports the binding of the anionic site of PBAs with surfactant. The synthesis of electrocatalysts was confirmed through FT-IR spectroscopy and the overlaid spectra of all catalysts are shown in Figure 2. The figure shows that synthesized electrocatalysts have all the characteristic peaks associated with PB-type systems. Cyanide stretching frequency is the distinctive feature of cyanide-based coordination compounds. All three compounds show sharp bands in the frequency range 2079-2093 $cm^{-1}$. The cyanide stretching frequency increases with the increase in the positive character of the metal. That is why it is slightly high for NiHCF and then for CoNiHCF. At about 1610 $cm^{-1}$ there is a sharp band that corresponds to OH bending due to water molecules trapped inside the structure. While at 3200-3500 $cm^{-1}$ a broadband represents OH stretch. At about 3000 $cm^{-1}$ there is a hump that is because of the C−H stretch due to the presence of CTAB. 1500-1000 $cm^{-1}$ is a fingerprint region, representing alkyl group bending. The band at 500 $cm^{-1}$ corresponds to M−C stretching.

The crystalline content and phase of the synthesized compounds, PXRD was performed, and the spectra are shown in Figure 3. The spectra reveal that all the samples are iso-structural with the PB crystal system, having a face-centered cubic lattice and Fm3m space group symmetry. All the characteristic 2θ peaks are in good agreement with the reference databases for NiHCF and CoHCF [21]. The slight shift of the peaks' positions can be attributed to the presence of CTAB. The comparative spectra further reveal that the crystallinity of trimetallic CoNiHCF is reduced compared to bimetallic PBAs.

To further study the morphology of the PBAs scanning electron microscopy was performed. It appears in the form of two-dimensional images exhibiting the structural properties of the PBAs. For CoNiHCF Figure 4 shows the regular plate-like structures with uniform growth as shown in the close image with a resolution of 2 µm. The EDX spectrum for CoNiHCF confirms the presence of given metal atoms and hints at the atomic ratio of metals (Figure 5). The proposed molecular formula based on the stoichiometric ratio of the metals is $Co_{1.4}Ni_{0.3}CTAB_{0.3}[Fe(CN)_6]\cdot nH_2O$.

### 3.2. Electrocatalytic performance

LSV plots of all the PBAs in the buffer of neutral pH i.e., 7 with a potential range of 0-1.5 V Vs Ag/AgCl at a scan rate of 50 mV $sec^{-1}$ were taken after IR compensation. From the graph, as shown in Figure 6 (a), we can say that the activity of NiHCF with CTAB is least toward water oxidation reaction. CoHCF with CTAB performs better towards water oxidation but the best results are obtained for CoNiHCF with CTAB giving the overpotential of 570 mV at 1 mA $cm^{-2}$ current density. This can be attributed to the amorphous nature of CoNiHCF with CTAB compared to the others, hence providing more surface area for the reaction to occur. A comparison of the overpotential and Tafel slope for all three materials is given in Table 1.

To check the reaction kinetics Tafel plots were drawn between log j vs. overpotential. The slope of

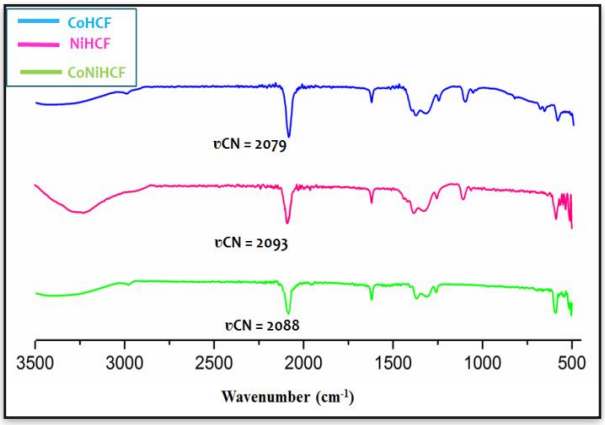


**Fig. 2.** Overlaid FT-IR spectra of synthesized electrocatalysts in the presence of CTAB.

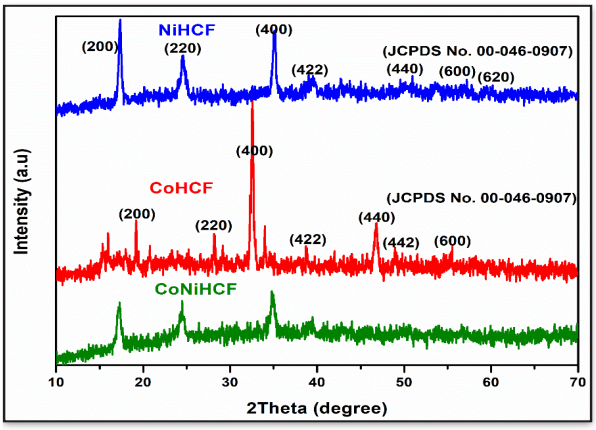


**Fig. 3.** PXRD patterns for all three synthesized PBAs.

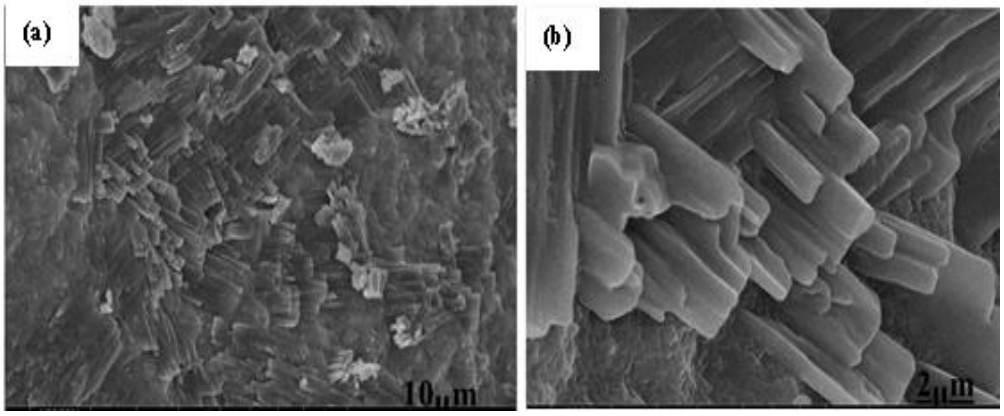


**Fig. 4.** SEM images of CoNiHCF at (a)10 μm and (b) 2 μm.

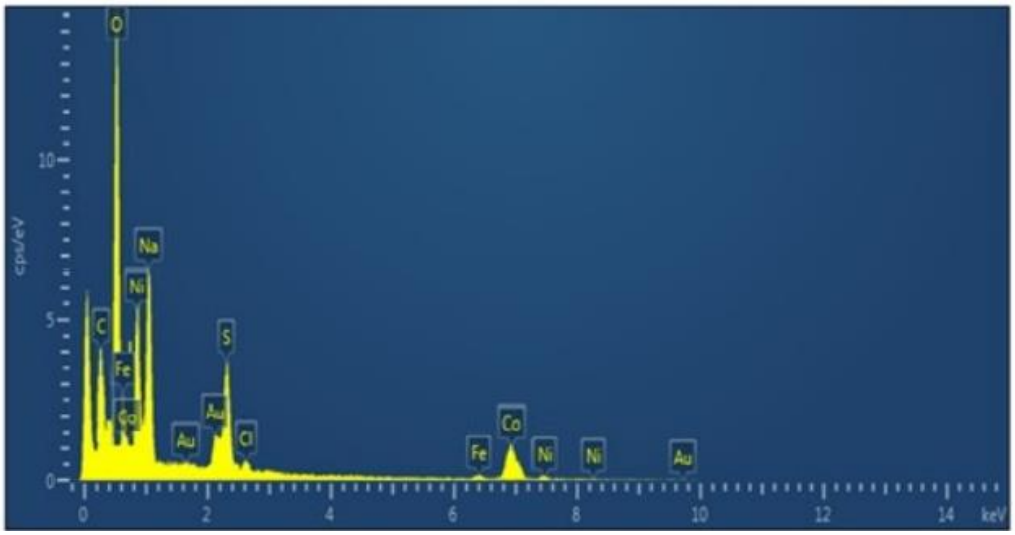


**Fig. 5.** EDX spectrum of CoNiHCF

the graph reflects reaction kinetics. The lower the Tafel slope, the faster will be the reaction kinetics. Figure 6 (b) shows the Tafel slope of all three compounds, where CoNiHCF has the lowest value of Tafel slope i.e., 133 mV/dec which indicates the fast reaction kinetics of trimetallic CoNiHCF for the water oxidation reaction considering more active sites on its surface than the other two bimetallic PBAs.

Cyclic voltammetry (CV) is used to measure the electrochemical surface area (ECSA) of the fabricated electrode in the non-faradic region by varying scan rates and the graph is shown in Figure 6 (c). It is clear from the graph that with the increasing scan rates the value of the current increases. From CV measurements, double-layer capacitance ($C_{dl}$) is calculated. The slope of the graph between scan rates ($mV.s^{-1}$) *vs.* the corresponding current (mA) provided double-layer capacitance as 45μF for CoNiHCF, (Figure 6 (d)). From the double-layer capacitance, ECSA reflecting the catalytic performance is determined. More active sites are reflected with higher ECSA possible electrochemical processes. ECSA is found to be 2.25 $cm^2$ for CoNiHCF. The ECSA further provides the roughness factor (RF) to be 32.1, associated with the electrocatalyst and is another important parameter to determine the catalytic efficiency. A

**Table 1.** Comparison of overpotential and Tafel slope for all three catalysts.

| Electrocatalysts | Overpotential (mV) @ 1 mA $cm^{-2}$ | Tafel slope (mV/dec) |
|---|---|---|
| **CoHCF** | 590 | 139 |
| **NiHCF** | 750 | 154 |
| **CoNiHCF** | 570 | 133 |

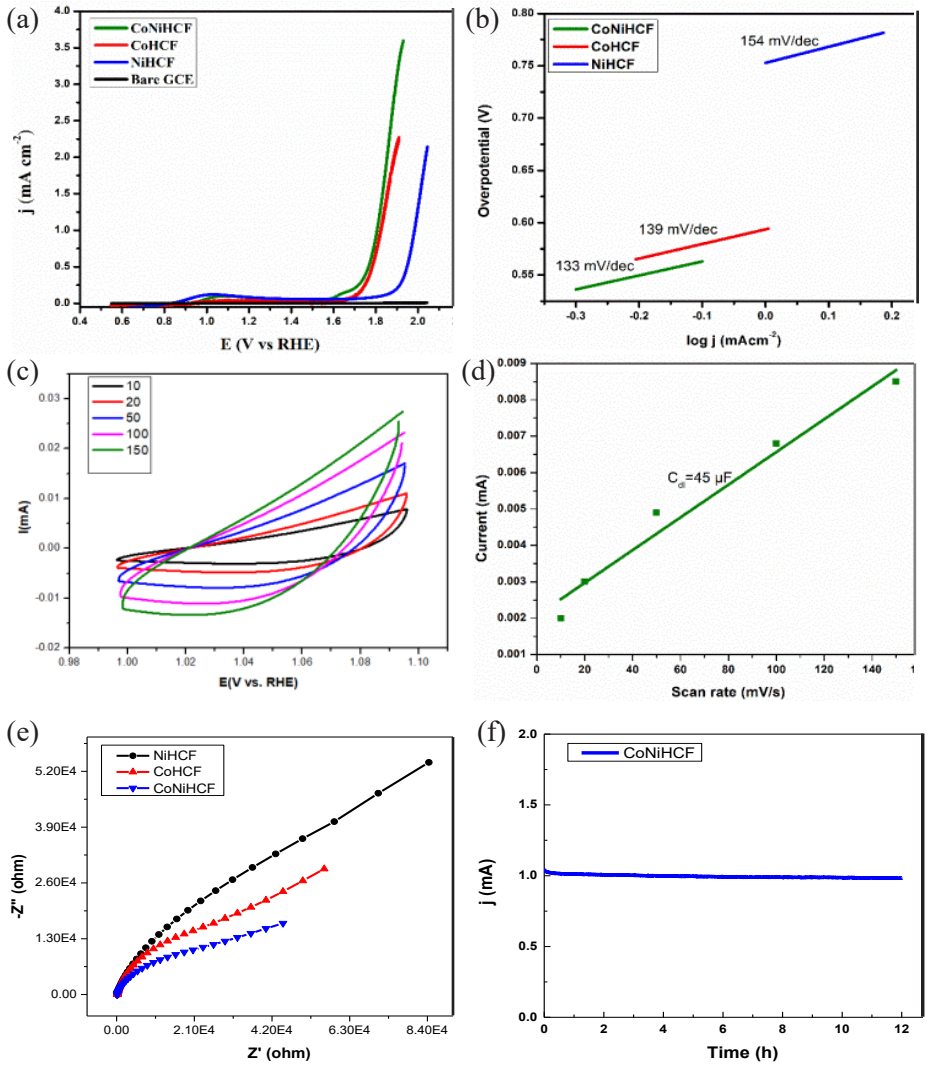


**Fig. 6** (a) LSV curves for all three synthesized PBAs compared with bare GCE, (b) Tafel plots of the three PBAs, (c) CV cycles in the non-faradaic region for CoNiHCF at scan rates varying from 10-150 mV $sec^{-1}$, (d) measurement of double-layer capacitance from changing current and scan rate plot for CoNiHCF, (e) Nyquist plots from 0.1Hz to 100KHz frequency range for all three PBAs, and (f) chronoamperometric stability plot at potential correlated with 1 mA $cm^{-2}$ current density for CoNiHCF.

high value of the RF means a more active surface and efficiency for the water oxidation mechanism. Electrochemical Impedance Spectroscopy is used to investigate the changes that take place in the interfacial properties of the electrode upon their encounter with the analyte species [22]. The plots in Figure 6(e) illustrated a smaller semicircle in the high-frequency region corresponding to the lower value of the charge transfer resistance ($R_{ct}$). CoNiHCF has a very efficient charge transfer process with a very small resistance because of which it has high water oxidation catalytic efficiency.

During the water oxidation process, the stability of the working electrode is tested by using chronoamperometry 1.8 V vs. RHE (constant potential) for the trimetallic CoNiHCF. The electrocatalyst produced a corresponding constant current density for 12 hours as shown in Figure 6 (f).

The comparison of electrochemical performance is given in Table 1. The data shows that the CoNiHCF has a lower overpotential and Tafel slope value which reflects more active sites

available for water oxidation. This can be attributed to the synergistic effect of the presence of Ni and Co, where both are available as active sites for the water oxidation process with faster kinetics and lower $R_{ct}$.

## 4. CONCLUSION

In this work, two bi-metallic and one tri-metallic PBAs were synthesized onto the surface of a glassy carbon electrode by applying surfactant-promoted in-situ approach to investigate their performance as heterogeneous electrocatalysts for OER. The presence of CTAB as a cationic surfactant ultimately enhances the electrochemical performances of the PBAs. The electrochemical water oxidation studies of all the fabricated electrodes were performed at neutral pH ($Na_3PO_4$ buffer, $NaNO_3$ as electrolyte). The electrode fabricated with CoNiHCF required the lowest overpotential of 570 mV compared to CoHCF (required 590 mV) and NiHCF (required 750 mV) to achieve the current density of 1 mA $cm^{-2}$. Tri-metallic CoNiHCF being a better catalyst than the other synthesized ones, showed an ECSA of about 2.25 $cm^2$ with a roughness factor of 32.1. The surfactant-assisted approach reported herein provides a binder-free strategy for fabricating PBA-based electrocatalysts over the electrodes and the approach can be expanded to other related materials and substrates as well.

## 5. ACKNOWLEDGEMENT

A.H. and S.A. are thankful to Pakistan Academy of Sciences for Financial support in the form of project funds (2020-22).

## 6. CONFLICT OF INTEREST

The authors declared no conflict of interest.

## 7. REFERENCES

1. M.I. Hoffert, K. Caldeira, A.K. Jain, E.F. Haites, L. Harvey, S.D. Potter, M.E. Schlesinger, S.H. Schneider, R.G. Watts, and T.M. Wigley. Energy implications of future stabilization of atmospheric $CO_2$ content. *Nature* 395: 881-884 (1998).
2. S. Chu, and A. Majumdar. Opportunities and challenges for a sustainable energy future. *Nature* 488: 294-303 (2012).
3. A. Mahmood, W. Guo, H. Tabassum, and R. Zou. Metal-organic framework-based nanomaterials for electrocatalysis. *Advanced Energy Materials* 6: 1600423 (2016).
4. M. Aksoy, S.V.K. Nune, and F. Karadas. A novel synthetic route for the preparation of an amorphous Co/Fe prussian blue coordination compound with high electrocatalytic water oxidation activity. *Inorganic Chemistry* 55: 4301-4307 (2016).
5. I. Roger, M.A. Shipman, and M.D. Symes. Earth-abundant catalysts for electrochemical and photoelectrochemical water splitting. *Nature Reviews Chemistry* 1: 1-13 (2017).
6. R. Liu, G. Zhang, H. Cao, S. Zhang, Y. Xie, A. Haider, U. Kortz, B. Chen, N.S. Dalal, Y. Zhao, L. Zhi, C. Wu, L. Yan, Z. Su, and B. Keita. Enhanced proton and electron reservoir abilities of polyoxometalate grafted on graphene for high-performance hydrogen evolution. *Energy and Environmental Science* 9: 1012-1023 (2016).
7. D. Durbin, and C. Malardier-Jugroot. Review of hydrogen storage techniques for on board vehicle applications. *International journal of hydrogen energy* 38: 14595-14617 (2013).
8. A. Kudo, and Y. Miseki. Heterogeneous photocatalyst materials for water splitting. *Chemical Society Reviews* 38: 253-278 (2009).
9. J. Zhang, Z. Zhao, Z. Xia, and L. Dai. A metal-free bifunctional electrocatalyst for oxygen reduction and oxygen evolution reactions. *Nature Nanotechnology* 10: 444-452 (2015).
10. D.F. Abbott, D. Lebedev, K. Waltar, M. Povia, M. Nachtegaal, E. Fabbri, C. Copéret, and T.J. Schmidt. Iridium oxide for the oxygen evolution reaction: correlation between particle size, morphology, and the surface hydroxo layer from operando XAS. *Chemistry of Materials* 28: 6591-6604 (2016).
11. W.T. Hong, M. Risch, K.A. Stoerzinger, A. Grimaud, J. Suntivich, and Y. Shao-Horn. Toward the rational design of non-precious transition metal oxides for oxygen electrocatalysis. *Energy & Environmental Science* 8: 1404-1427 (2015).
12. M.W. Kanan, and D.G. Nocera. In situ formation of an oxygen-evolving catalyst in neutral water containing phosphate and $Co^{2+}$. *Science* 321: 1072-1075 (2008).
13. I. Ullah, A. Munir, A. Haider, N. Ullah, and I. Hussain. Supported polyoxometalates as emerging nanohybrid materials for photochemical and photoelectrochemical water splitting. *Nanophotonics* 10(6): 1595-1620 (2021).
14. R. Khan, J. Arshad, S. Khan, M.A. Mansoor, S. Ali, T. Nisar, V. Wagner, M.A. Asghar, and A. Haider. Surfactant-assisted fabrication of prussian blue analogs as bifunctional electrocatalysts for water and hydrazine oxidation. *Molecular Catalysis* 548: 113415 (2023).
15. S. Goberna-Ferron, W.Y. Hernandez, B. Rodriguez-Garcia, and J.R. Galán-Mascarós. Light-driven water oxidation with metal hexacyanometallate heterogeneous catalysts. *ACS Catalysis* 4: 1637-

1641 (2014).
16. L. Han, P. Tang, A. Reyes-Carmona, B. Rodríguez-García, M. Torréns, J.R. Morante, J. Arbiol, and J.R. Galán-Mascarós. Enhanced Activity and Acid pH Stability of Prussian Blue-type Oxygen Evolution Electrocatalysts Processed by Chemical Etching. *Journal of American Chemical Society* 138: 16037-16045 (2016).
17. L. Han, and J.R. Galán-Mascarós. The Positive Effect of Iron Doping in the Electrocatalytic Activity of Cobalt Hexacyanoferrate. *Catalysts* 10: 130 (2020).
18. F.S. Hegner, F.A. Garcés-Pineda, J. González-Cobos, B. Rodríguez-García, M. Torréns, E. Palomares, N. López, and J.R. Galán-Mascarós. Understanding the Catalytic Selectivity of Cobalt Hexacyanoferrate toward Oxygen Evolution in Seawater Electrolysis. *ACS Catalysis* 11: 13140–13148 (2021).
19. Ruqia, M.A. Asghar, S. Ibadat, S. Abbas, T. Nisar, V. Wagner, M. Zubair, I. Ullah S. Ali, and A. Haider. Binder-free fabrication of Prussian blue analogues based electrocatalyst for enhanced electrocatalytic water oxidation. *Molecules* 27: 6396 (2022).
20. Y. Feng, X. Wang, P. Dong, J. Li, L. Feng, J. Huang, L. Cao, L. Feng, K. Kajiyoshi, and C. Wang. Boosting the activity of Prussian-blue analogue as efficient electrocatalyst for water and urea oxidation. *Scientific Reports* 9: 1-11 (2019).
21. H.T. Ashfaq, M.A. Asghar, T. Nisar, V. Wagner, M.A. Mansoor, A. Haider, and S. Ali. Electrochemical Synthesis of CoNi- and NiCo-Based hexacyanocobaltates as efficient electrocatalysts for water oxidation studies. *Inorganic Chemistry Communications* 154: 110916 (2023).
22. B.Y. Chang, and S.M. Park. Electrochemical impedance spectroscopy. *Annual Review of Analytical Chemistry* 3: 207 (2010).